

Improvement on Infrared Imaging Video Bolometer by Laser Calibration Method^{*})

Muneji ITOMI, Byron J. PETERSON¹⁾, Yuji YAMAUCHI²⁾, Ryuichi SANO³⁾,
Kiyofumi MUKAI¹⁾ and Shwetang N. PANDYA³⁾

Graduate School of Engineering, Hokkaido University, Kita-13, Nishi-8, Kita-ku, Sapporo 060-8628, Japan

¹⁾*National Institute for Fusion Science, 322-6 Oroshi-cho, Toki 509-5292, Japan*

²⁾*Faculty of Engineering, Hokkaido University, Kita-13, Nishi-8, Kita-ku, Sapporo 060-8628, Japan*

³⁾*Graduate University for Advanced Studies Department of Fusion Science, 322-6 Oroshi-cho, Toki 509-5292, Japan*

(Received 10 December 2013 / Accepted 29 March 2014)

It is necessary to estimate and decrease energy losses while keeping a high performance plasma in a nuclear fusion reactor. Therefore radiation diagnostics are required to estimate the radiation loss as a part of the total energy loss. Our diagnostic, the InfraRed imaging Video Bolometer (IRVB), which has been used in Large Helical Device (LHD), JT-60U and KSTAR, measures the radiation loss from the plasma. First, a metal foil, which is part of the diagnostic, absorbs radiation energy through an aperture and its temperature rises due to this energy. An IR camera measures the 2D distribution of the temperature on the foil, then we obtain the irradiance intensity and distribution by solving the heat diffusion equation on the foil. The purpose of our study is the development of the foil calibration analysis with laser for measuring plasma radiation with an IRVB using a Finite Element Model (FEM). This paper shows the improvement from two viewpoints. The first one is from the spatial resolution, and second one is the addition of the time dependent part in the heat diffusion equation with the IRVB calibration of the foil thermal diffusivity.

© 2014 The Japan Society of Plasma Science and Nuclear Fusion Research

Keywords: Large Helical Device, infrared imaging, plasma diagnostics, IRVB, finite element model, laser calibration

DOI: 10.1585/pfr.9.3406080

1. Introduction

An InfraRed imaging Video Bolometer (IRVB) [1] is a measurement instrument for plasma radiation. It is useful for the measurement of both radiation intensity and spatial distribution. These measurement data are useful for the operation of a fusion device. IRVBs have been used in LHD [1] and JT-60U [2] etc. with a bolometer foil. Figure 1 shows the schematic of the IRVB principle. An IRVB foil absorbs the plasma radiation through an aperture and the resulting temperature distribution on the metal foil, which is measured by an IR camera, is used to calculate the absorbed radiation.

Some spatial non uniformities occur in the physical and thermal parameters of the foil which determine the heat diffusion in the foil. Then, calibration is needed to compensate for these non uniformities in the heat diffusion equation of the metal foil when it receives the plasma radiation and emits the IR irradiation to the IR camera. The parameters are the thickness of metal foil, t_f , and the emissivity, ϵ , in steady state, as we discuss later. In addition, there is the thermal diffusion coefficient, κ , as a parameter in non-steady state.

author's e-mail: itomi_muneji@frontier.hokudai.ac.jp

^{*}) This article is based on the presentation at the 23rd International Toki Conference (ITC23).

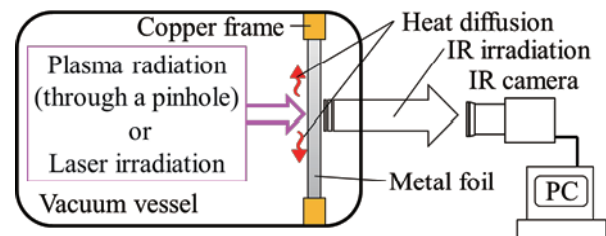


Fig. 1 The schematic of an IRVB. IRVB acquires the irradiance power to the metal foil using calibration parameters. In the laser calibration experiment, the incident laser replaces the plasma radiation.

Here, these parameters are obtained for each bolometer pixel area into which the foil is divided. In the past study [3] each area is defined as a square of 1 cm one side, on the other hand we researched the influence of higher spatial resolution if one side is 5mm. Spatial resolution is important because better spatial resolution will be needed in the future to measure the radiation from local phenomenon like the magnetic island and near the diverter tiles in the case of detached plasma.

Additionally, the time derivative term in the heat diffusion equation was ignored in the previous calibration

method. Therefore we investigated the influence of adding the time derivative term. That let the measurement of radiation in short time spans is possible.

2. Devices and Method

2.1 IRVB and heat diffusion equation

The main device is an IRVB, and ANSYS is used as a Finite Elemental Method (FEM) simulation tool in the heat diffusion.

Figure 1 shows the schematic of an IRVB. It is composed primarily of a metal foil and an IR camera. The metal foil receives the plasma radiation (or laser irradiation during the laser calibration experiment) power, after that the temperature of the location radiated rises. The IR radiation to the IR camera is emitted from the back of the metal foil corresponding to the temperature on the foil. At that time, the phenomenon obeys the heat diffusion equation,

$$-\Omega_{\text{rad}} + \Omega_{\text{bb}} + \frac{1}{\kappa} \frac{\partial T}{\partial t} = \frac{\partial^2 T}{\partial x^2} + \frac{\partial^2 T}{\partial y^2}, \quad (1)$$

$$\text{where } \Omega_{\text{bb}} = \frac{\varepsilon \sigma_{\text{SB}} (T^4 - T_0^4)}{kt_f}, \quad \Omega_{\text{rad}} = \frac{P_{\text{rad}}}{kt_f}$$

$$\text{and } \kappa = \frac{k}{c\rho}. \quad (2)$$

Here, the heat transfer to air is ignored because the foil is at high vacuum in the vessel. T is the two-dimensional temperature distribution on the foil measured by the IR camera, k is the foil thermal conductivity, t_f is the thickness of the metal foil, σ_{SB} is the Stefan-Boltzmann constant, ε is the black body emissivity, T_0 is the background temperature, P_{rad} is the incident radiation power density, c is the thermal capacity and κ is the thermal diffusivity of the foil. In past studies [3] the term including κ has not been estimated in Eq. 1 because the method is considered in the steady state only.

The standard thickness of a metal foil for LHD is $2.5 \mu\text{m}$ that is decided by the maximum photon energy from the LHD plasma to be measured [2]. This foil is made of Pt, the size is $9 \text{ cm} \times 7 \text{ cm}$. Both of the foil surfaces are blackened by graphite coating for the purpose of raising the radiation emissivity on the surface. The metal foil is fixed to four sides of the chamber by Cu frames.

In this study, the IR camera (FLIR/SC4000) is used. The spectral range is $3 \sim 5 \mu\text{m}$, the maximum shutter speed is 100fps and the resolution is 320×256 pixels.

2.2 Other devices

The temperature is room temperature, and the pressure in the vacuum vessel is about $< 1 \text{ mTorr}$ which makes heat transfer from metal foil to the air altogether negligible.

The power of the He-Ne laser is 10 mW, and the measured beam diameter is 0.6 mm during the experiment. The metal foil is irradiated at each point in turn while meandering as shown in Fig. 2.

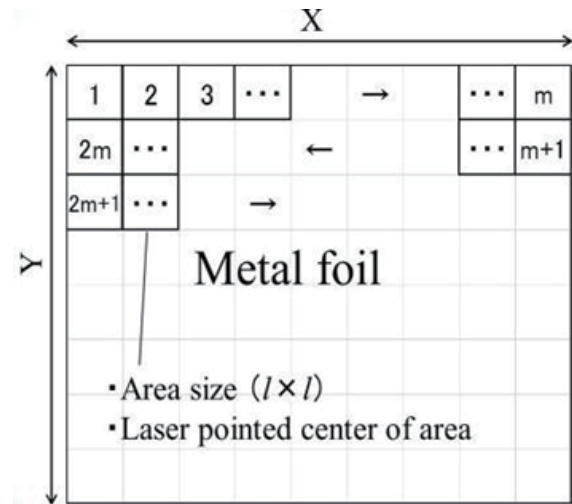


Fig. 2 The detail of the position irradiated by the laser on the metal foil. $X = 9 \text{ cm}$, $Y = 7 \text{ cm}$. IRVB pixel size is changed from $l = 1 \text{ cm}$ to $l = 5 \text{ mm}$ in this study.

2.3 Calibration method

The conventional method [3] used the following procedure. (a) The laser irradiation of known power, P_{rad} , is used in the laser experiment instead of the incident plasma radiation. Next, the laser experiment is simulated by an FEM. (b) The effective thickness of the metal foil, t_f , and (c) the effective emissivity are estimated in an iterative calculation by comparing both results of laser experiment and simulation. (d) The processes (b)~(c) are replicated to converge to the estimated values.

A new method is established considering the non-steady state term in the heat diffusion equation through the use of t_f and ε from an estimation in steady state. In addition to the above procedure, (e) the temperature decay data on the foil is gotten at non-steady state after the laser irradiated to steady state. The temperature decay is obeyed Eq. 3 while τ is the time constant.

$$T = \Delta T \left[\exp\left(-\frac{\sqrt{t}}{\tau}\right) \right] + T_0. \quad (3)$$

(f) The heat diffusion coefficient κ is estimated in the non-steady state calculation used τ . In this case, the variable parameter used at FEM in the iterative calculation is the density ρ shown in Eq. 2 while c is considered constant. (g) The calculation is replicated until the estimated value of ρ converges.

3. Results and Discussion

3.1 Influence of high spatial solution

Figure 3 and Fig. 4 show the relation between the temperature rise and position from the center of the IRVB pixel which is the laser irradiating point. The area of the foil is divided into a grid of 1 cm on a side in the case of Figs. 3, and 5 mm in the case of Fig. 4. Here, the data which is plotted as triangles indicates the FEM value that is adjusted

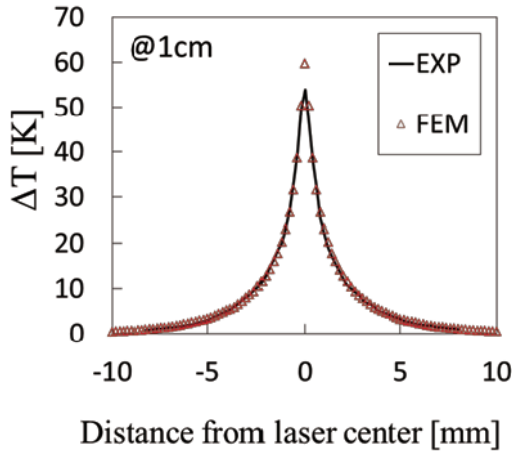


Fig. 3 The temperature profiles on the metal foil in the laser experiment and in the FEM simulation with a mesh dimension of 1 cm on a side. The triangle mark shows the peak value with FEM.

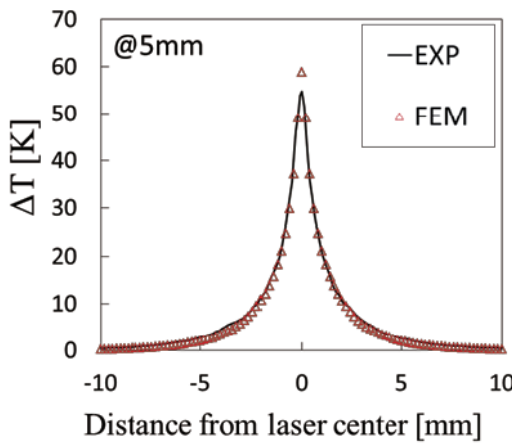


Fig. 4 The case of a 5 mm pixels dimension.

using Eq. 4 (Eq. 2 in Ref. 3) to the experimental temperature with the maximum temperature ΔT_{\max} and the width between the points $1/e$ of maximum temperature w , curvature of the peak fac .

$$T = T_0 + \Delta T_{\max} \exp\left(-\frac{\left(\left(\frac{x}{w}\right)^2\right)^{fac}}{2}\right). \quad (4)$$

There is a high coincidence between the experimental data and the adjusted simulation data in these figures. In this adjustment the different at top of curve because of the distribution inside of laser in experiment.

The comparing is based on the determined number R^2 applied least square method indicating degree of coincidence. In the case R^2 is near 1 that shows the 2 parameters get high coincidence. Table 1 show the R^2 from some areas at 1 cm model and 5 mm model. From the table the simulation model can be said to well reproduce the experiment. A difference is not observed in that, for example, there is a

Table 1 The determined numbers picked from 3 areas.

Irradiated location	$R^2@1\text{cm}$	$R^2@5\text{mm}$
A corner of foil	0.9957	0.9931
An edge of foil	0.9943	0.9948
A center of foil	0.9948	0.9943

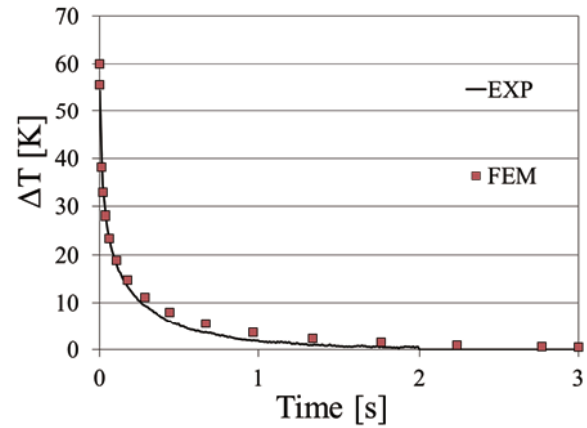


Fig. 5 The decrease of the temperature with time. The line is from the laser experiment, and the square plots from the FEM.

big mismatch between the data for $l = 5 \text{ mm}$ and $l = 1 \text{ cm}$. This result shows that as the spatial resolution is increased, it is possible to calibrate for a smaller pixel size. There is a point about which one must be careful when using this method. The smaller the area one uses, the more calculation time is needed. Considerations about the number of iterations and the area size are needed if the distances of some calibrations on the metal foil in once experiment term of plasma confinement device like LHD are short.

3.2 Influence of adding the time derivative term

The time derivative term is included to the heat diffusion equation but it is not considered for the existing model. It is clear that the measurement precision improves because a new term is added that is not considered in the past studies if the model has high reproducibility. The reproducibility needs to be considered in this study.

The condition of the laser irradiation is that firstly it is irradiated until it reaches as a steady state, after that it is shuttered. Figure 5 shows a plot of the time dependence of the temperature at a location with the laser irradiation after it was shuttered. The line shows the decreasing temperature in the experiment, and the diamond symbols show the FEM simulation. Both plots are almost identical. Each determined value is about 0.93 of the value of the previous iteration at the selected representative points in the foil, which are at the corner, the edge and the central parts. This suggests that the model has great reproducibility, because if the value is near 1.0, the reproducibility is higher. The time constant τ is obtained from a fit to the decay plot in

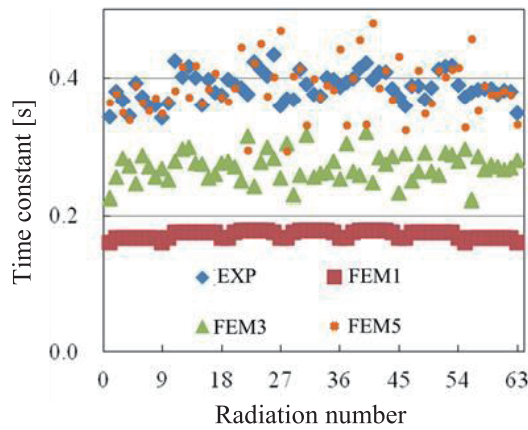


Fig. 6 These plots show the time constants from the laser experiment and from the FEM. The labeled numbers mean the number of the iterative calculation.

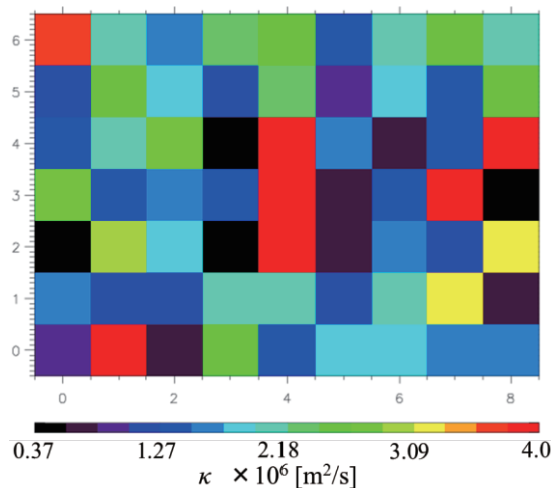


Fig. 7 Distribution of κ on the metal foil at 5th iterative calculation.

Eq. 3. After several iterations the FEM time constant converges to the experimental one and then, the density, ρ , is obtained.

Next, Fig. 6 shows the time constants that are ob-

tained from the laser experiment and the values estimated by FEM analysis. As stated already, the values are estimated by the iterative calculation five times. Thus the new model with the time derivative term has an effect on the IRVB calibration because the values of time constants and the curve in Fig. 5 are close between FEM and experiment. The values of the time constants in the FEM converge gradually to the experimental one by iterative calculation. In this case, the distribution of the thermal diffusivity κ on the metal foil at 5th iterative calculation is shown in Fig. 7.

4. Conclusion

This paper reports on the improved methods using FEM analysis in the IRVB calibration. The calibration obtains the mean thermal parameter distribution connected between the irradiated power and the temperature distribution formed on the metal foil using the heat diffusion equation including both steady state and non-steady state terms. Thus these results are obtained by this paper.

At first, the spatial resolution can be greater in the IRVB calibration in the model with a smaller pixel. That allows us measure the local radiation. In this case, we must be careful about the amount of time for the iteration analysis.

At second, this study suggested that the calibration with high accuracy is enabled because the time derivative term in the heat diffusion equation is added to the past model. Also the simulation model has high reproducibility. Thus the result shows the possibility that we can measure the radiation in short time spans.

Acknowledgement

This research is carried out with the support of NIFS budget NIFS12ULHH026 and NIFS collaboration budgets NIFS 12KLEH015 and NIFS12KEKO002.

[1] B.J. Peterson *et al.*, Rev. Sci. Instrum. **74**(3), 2040 (2003).
 [2] B.J. Peterson *et al.*, Rev. Sci. Instrum. **77**(10E515), S2095 (2006).
 [3] R. Sano *et al.*, Plasma Fusion Res. **7**, 2405039 (2012).